Structural Aspects of RecA-Dependent Homologous Strand Exchange Involving Human Telomeric DNA†

Sima S. Zein‡ and Stephen D. Levene*,‡,§

Department of Molecular and Cell Biology and Institute of Biomedical Sciences and Technology, University of Texas at Dallas, Richardson, Texas 75083

Received October 22, 2004; Revised Manuscript Received December 20, 2004

ABSTRACT: Telomeric DNA sequences in human cells and those of other vertebrates consist of long d(TTAGGG) repeats. In somatic cells, telomeres shorten every cell division with shortening serving as a mitotic clock that counts cell divisions and ultimately results in cellular senescence. Telomere length is principally maintained by a ribonucleoprotein, telomerase. However, a non-negligible proportion of human cells use a recombination-based mechanism for telomere maintenance, termed alternative maintenance of telomeres (ALT). Although the molecular mechanism of ALT is not known, GT-rich sequences in prokaryotes and eukaryotes display high levels of recombination relative to those of non-GT-rich DNA. We show that human telomeric strand-exchange complexes mediated by *Escherichia coli* RecA protein differ from those formed with nontelomeric sequences. Moreover, telomeric strand-exchange intermediates, unlike those involving nontelomeric sequences, exhibit a tendency to form higher-order nucleoprotein structures. We propose that the strong DNA unwinding activity inherent in the assembly of the RecA strand-exchange complex promotes the formation of alternative DNA structures at human telomeric loci. Organization of these noncanonical structures into higher-order complexes involving multiple DNA duplexes could facilitate the search for homology on different DNA molecules and provide a framework for understanding recombination-dependent mechanisms of telomere maintenance.

The *Escherichia coli* RecA system provides a valuable paradigm for the complex mechanisms of homologous recombination. In the presence of ATP, or its slowly hydrolyzable form, ATPγS,[1] the RecA strand-exchange protein binds to single-stranded DNA to form a right-handed nucleoprotein filament (*1*, *2*). Subsequently, the nucleoprotein filament searches for homologous sequences on target duplex DNA, followed by pairing of the incoming strand and its complement and displacement of the noncomplementary single strand.

Molecular details of the search for DNA homology and subsequent homologous pairing are not well understood. Previous studies showed that during pairing of ssDNA and dsDNA, the triple-stranded intermediate that forms has the typical helical parameters of the RecA filament, where all strands are stretched and underwound to give a helical repeat of 18.6 residues per helical turn (*3*−*5*). The triple-stranded intermediate consists of a newly formed duplex in which the incoming single strand is base paired with its complement from the original duplex and the nascent displaced strand is wound around the newly formed duplex region (*4*). The stretching of all DNA strands in the complex is believed to be necessary to expose the DNA bases in a manner required for homologous pairing interactions (*6*−*8*).

Homologous recombination strand-exchange proteins are characterized by their ability to bind DNA in a sequence-independent manner and to pair any homologous DNA sequence with its partner (*9*). Similar fundamental mechanisms are the basis for homologous strand exchange in bacteria, yeast, and humans. RecA and its homologue in *Saccharomyces cerevisiae*, Rad51, have preferential affinity and enhanced pairing activity with GT-rich DNA sequences (*10*, *11*). In prokaryotes and eukaryotes, genomic loci containing GT-rich sequences show enhanced levels of recombination. Examples of such sequences are the *E. coli* hot spot Chi (χ, 5′-GCTGGTGG-3′) (*12*), short tandemly repeated motifs in human and mammalian systems known as "satellite DNA" (*13*), CTG·CAG repeat sequences (*14*), and subtelomeric and telomeric sequences in yeast and human cells that use homologous recombination-based pathways for their maintenance (*15*, *16*).

Telomeres, the GT-rich DNA sequences located at the ends of eukaryotic chromosomes, have received considerable attention due to the fact that these structures are the substrate for the ribonucleoprotein telomerase, which is active in the vast majority of tumor cells, but not present in normal somatic cells (*17*). One strategy for treating malignant tumors is to inhibit the lengthening of telomeres in neoplastic cells by targeting telomerase activity (*18*). Recently, another mechanism for telomere lengthening has been investigated, termed alternative lengthening of telomeres (ALT). This

† Supported by a grant (GM55871) to S.D.L. from the National Institutes of General Medical Sciences of the National Institutes of Health.

* To whom correspondence should be addressed. Telephone: (972) 883-2503. Fax: (972) 883-2486. E-mail: sdlevene@utdallas.edu.

‡ Department of Molecular and Cell Biology.

§ Institute of Biomedical Sciences and Technology.

[1] Abbreviations: ALT, alternative lengthening of telomeres; ECTR, extrachromosomal telomeric repeat; ATPγS, adenosine 5′-*O*-(3-thio)-triphosphate; DMS, dimethyl sulfate.

10.1021/bi047735r CCC: $30.25
Published on Web 03/02/2005

A.

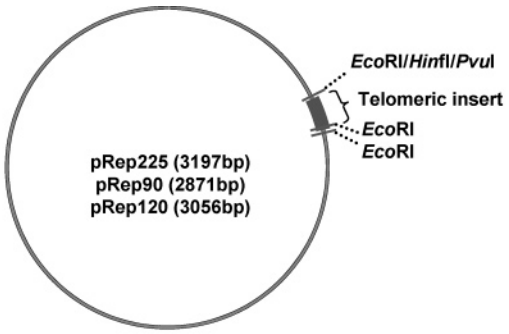

B.

Plasmid	Telomeric insert
pRep90	$(T_2AG_3)_{16}T_2AG$
pRep120	$(T_2AG_3)_{23}T_2A$
pRep225	$(T_2AG_3)_{35}T_2A$

C.

223-nt G-rich	$AATTC(T_2AG_3)_{35}T_2AGAATT$
151-nt G-rich	$ACTCG(T_2AG_3)_{23}T_2AGAATT$
100-nt G-rich	$(T_2AG_3)_{16}T_2AG$
151-nt C-rich	$AATTCTA_2(C_3TA_2)_{23}CGAGT$
100-nt C-rich	$CTA_2(C_3TA_2)_{16}$
100G58N5'	GACAGGGCGCGTCCCATT CGCCATTCAGGCTGCGCA ACTGTTGGGAAGGGCGAT $CGGG(T_2AG_3)_{16}AATT$
100G58N3'	$CGGG(T_2AG_3)_{16}$AATTCGGC CGCGGCCGAATTCCTGCA GCCCGGGGGATCCACTAG TTCTAGAGCGGCCG

FIGURE 1: Sequences of telomeric repeat DNAs. (A) pRep90 and pRep120 were derived by λ-exonuclease digestion of pRep225 (see Experimental Procedures). All three plasmids have an *Eco*RI recognition site that is part of the 3′-end of the G-rich sequence of the telomeric insert, separated from an additional downstream *Eco*RI site by 10 bp. *Eco*RI, *Hin*fI, and *Pvu*I restriction sites are located at similar positions in pRep90, pRep120, and pRep225, respectively, upstream of the telomeric insert. (B) Sequences of telomeric inserts in the plasmid DNAs described in panel A. (C) Sequences of single-stranded constructs prepared as described in Experimental Procedures.

mechanism is independent of telomerase activity and dependent on homologous recombination. ALT-dependent telomere maintenance can coexist with telomerase activity in certain tumor cells, and as a consequence, control of telomere lengthening in such cells will be less sensitive to anti-telomerase drugs (*19*). Human ALT cells have been characterized by the presence of novel nuclear structures called ALT-associated PML bodies (APBs) (*20*). APBs contain short fragments (approximately 1 kb) of telomeric DNA [extrachromosomal telomeric repeats (ECTRs)] in addition to telomere binding proteins, proteins involved in homologous recombination (Rad51 and Rad52), and proteins involved in DNA damage repair (*20*−*22*).

E. coli RecA protein and Rad51, its eukaryotic homologue from yeast or human sources, have similar properties. The Rad51 nucleoprotein filament has virtually the same structure as that reported for RecA (*23*, *24*), and Rad51-dependent strand-exchange steps in recombination have been shown to be very similar to the reactions carried out by RecA protein (*25*−*28*). In this study, we examined topological aspects of RecA protein-mediated strand-exchange intermediates formed by human telomeric DNA $(TTAGGG)_n$ sequences (*29*). Remarkably, strand-exchange complexes involving telomeric single strands show a propensity to form higher-order structures, behavior that is not observed using nontelomeric single strands. We suggest the possibility that the enhancement of recombination observed with telomeric sequences in ALT cells may be due to the formation of higher-order strand-exchange complexes involving more than one telomeric duplex, thereby increasing the efficiency of homologous recombination at telomeric loci.

EXPERIMENTAL PROCEDURES

Plasmid DNA. Plasmid DNAs were derivatives of pRep225 BSK+, which contains 35 tandem copies of the human telomeric sequence, d(TTAGGG), and was a gift from W. Wright and J. Shay (University of Texas Southwestern School of Medicine, Dallas, TX; see Figure 1). Several plasmids with shorter telomeric sequences were generated, two of which were used in this study [pRep120 ($[T_2AG_3]_{23}T_2A$) and pRep90 ($[T_2AG_3]_{16}T_2AG$); see also Figure 1A,B]. These plasmids were generated by limited digestion with λ-exonuclease (Roche) of pRep225 BSK+, which was linearized at a unique *Eco*RV site located 18 bp from one end of the telomeric insert. Exonuclease-treated plasmids were digested with S1 nuclease (Roche), and blunt-end ligation was carried out with T4 DNA ligase (New England Biolabs). Transformants were screened for the length of telomeric repeat inserts, and insert sequences were confirmed by dideoxy DNA sequencing. All plasmids were propagated in *E. coli* SURE cells (Stratagene) grown at 30 °C to maintain insert stability. Plasmid DNA was isolated by an alkaline lysis procedure and purified by precipitation with polyethylene glycol (*30*). Insert sequences were confirmed by dideoxynucleotide sequencing for every plasmid preparation. To eliminate contributions from higher-order DNA structures that tend to accumulate with prolonged storage of telomeric DNA molecules, monomeric forms of the plasmid were purified prior to each series of experiments and used within 24 h.

Single-Stranded DNA Fragments. Three 100-nucleotide single-stranded DNA fragments ($[T_2AG_3]_{16}T_2AG$, $CTA_2[C_3TA_2]_{16}$, and a 100-nucleotide nontelomeric DNA sequence homologous to a 100-nucleotide region of pRep225 BSK+) were synthesized commercially (IDT) and purified sequentially by ion-exchange HPLC and denaturing polyacrylamide gel electrophoresis. All other single-stranded molecules were prepared by asymmetric PCR methods. The telomeric repeat-bearing plasmids pRep225 BSK+ and pRep120 were used as templates in symmetric PCR mixtures containing appropriate forward and reverse primers suitable for amplifying

the telomeric inserts. Nontelomeric ssDNA controls were derived from selected regions of pRep225 BSK+ using appropriate primers. PCR mixtures (50 μL) were subjected to 40 cycles of amplification in high-fidelity PCR buffer (Invitrogen) containing 0.2 mM dNTPs, 0.2 μM primer, 1.5 mM $MgSO_4$, and 1.5 units of Platinum Taq (Invitrogen). Extraneous vector DNA at the 3′-end of the G-rich repeat strand was removed from the symmetric PCR products by digestion with *Eco*RI. The double-stranded repeat-bearing DNAs were then used as templates to amplify the G-rich or C-rich telomeric repeat strand. These reactions were carried out under reaction conditions identical to those of symmetric PCR, but the mixtures contained only a single forward primer. The single-stranded product was isolated by gel electrophoresis, and sequences were confirmed by dideoxy DNA sequencing. The purity of the ssDNA molecules prepared by this method equaled or exceeded that of shorter ssDNA fragments that were prepared by oligonucleotide synthesis and underwent two rounds of PAGE purification (S. S. Zein, A. Vetcher, and S. D. Levene, manuscript submitted for publication).

RecA-Dependent Strand Invasion Assay. Single-stranded DNA samples in TE buffer [10 mM Tris-HCl and 1 mM Na_2EDTA (pH 8.0)] were denatured by heating to 95 °C in a thermal cycler for 5 min and cooling in situ to 25 °C. Denatured ssDNA was incubated with RecA (Roche) at a ratio of 5:3 (moles of nucleotides to moles of RecA) in buffer consisting of 20 mM triethanolamine-HCl (pH 7.2), 1 mM magnesium acetate, 1 mM DTT, and 2 mM ATPγS (Sigma) for 60 min at 37 °C. Presynaptic complexes were separated from RecA monomers by Sepharose CL-4B (Sigma) spin column chromatography using columns that were pre-equilibrated with 20 mM triethanolamine-HCl (pH 7.2), 1 mM magnesium acetate, and 1 mM DTT. ATPγS was added to a final concentration of 2 mM to fractions containing the RecA−ssDNA complexes. Presynaptic complexes were mixed at a 5-fold molar excess with homologous plasmid DNA relaxed by treatment with wheat germ topoisomerase I (Promega). The magnesium acetate concentration was adjusted to 6 mM, and the pairing reaction was allowed to continue at 37 °C for 2 h. Topoisomerase I (10 units/μg of plasmid DNA) was added, and the relaxation reaction was allowed to proceed for 1 h. Proteins were removed by treatment with SDS (final concentration of 0.1%) followed by two extractions with phenol, and DNA was recovered by ethanol precipitation. Topoisomers were analyzed by electrophoresis in 1.3% agarose gels for 24 h in TBE buffer [50 mM Tris-borate and 1 mM Na_2EDTA (pH 8.3) at 22 °C] containing from 0 to 1.1 μg/mL chloroquine phosphate. In many experiments, multiple gels containing different concentrations of chloroquine were used to fully characterize topoisomer distributions. After staining with ethidium bromide had been carried out, gel images were collected with a MicroMax Peltier-cooled, 12-bit (1:4096) CCD camera (Princeton Instruments) having a spatial resolution of 1317 × 1024 pixels.

Methylation Protection Assays. One hundred-nucleotide G-rich telomeric ssDNA or a 158-nucleotide sequence-containing G-rich repeats and a 58-nucleotide 3′-nontelomeric sequence extension (designated 100G58N3′; see Figure 1C) were paired with pRep90 under our standard strand-exchange assay conditions. Reaction mixtures were removed to 20 °C; dimethyl sulfate (Acros Organics) was added to a final concentration of 0.24%, and incubation continued for an additional 5 min. Methylation was terminated by chilling the reaction mixtures on ice and adding 0.1 volume of 10× DMS stop solution [3 M sodium acetate (pH 7.0), 0.2 M β-mercaptoethanol, and 10 μg/mL glycogen] followed by precipitation with ethanol. DNA was resuspended in 0.1% SDS, sequentially extracted with phenol, phenol and chloroform (1:1), and chloroform, and recovered by ethanol precipitation. Plasmid DNAs were digested at a unique *Not*I site and labeled with [α-^{32}P]dGTP (ICN) by using Klenow fragment (New England Biolabs). The plasmids were then digested with appropriate restriction endonucleases to remove the redundant labeled end. Samples were chemically cleaved at methylated sites by treatment with a 1 M solution of freshly diluted piperidine (Sigma-Aldrich) at 90 °C for 30 min. Reaction mixtures were analyzed on an 8% denaturing polyacrylamide gel.

RESULTS

Topological Assays of Single-Strand Invasion. We examined topological aspects of single-strand invasion in telomeric sequences by using plasmid DNAs subjected to RecA-mediated strand exchange involving homologous telomeric or nontelomeric single-stranded DNA sequences. These experiments are based on a variation of the classic nucleosomal linking-number experiment, in which a change in a plasmid's linking number (*Lk*), or topoisomer, distribution is induced by the binding of a ligand (*31*, *32*). Covalently closed DNAs are relaxed by topoisomerase I in the presence and absence of the ligand, and these two samples are subjected to agarose gel electrophoresis (Figure 2). If ligand binding perturbs DNA twist, then the distribution of plasmid topoisomers obtained for the ligand−DNA complex is shifted relative to the distribution observed in the absence of the ligand. In the case of ligand-induced DNA unwinding, the center of the *Lk* distribution observed for the topoisomerase-relaxed complex after removal of the ligand will reveal a linking number deficit ($\Delta Lk < 0$) relative to the relaxed plasmid alone.

On the basis of this principle, changes in the linking number distributions of plasmid DNAs that contain known repeat lengths of the human telomeric sequence, $d(TTAGGG)_n$, were used as a reporter for single-strand invasion in an assay involving homologous (either G strand or C strand) telomeric repeat-containing single strands. Incubation of these ssDNAs with RecA protein generates stable ssDNA−RecA filaments, which bind to homologous regions in plasmid DNA as a paranemic-joint complex, a structure in which DNA strands are paired, but not topologically linked (*33*, *34*). Relaxation of this complex with topoisomerase I, removal of RecA and ssDNA, and subsequent agarose gel electrophoresis in the presence of an intercalating agent have been previously shown to generate pronounced shifts in plasmid topoisomer distributions with nontelomeric DNA sequences (*4*, *35*).

Topoisomer Distributions. We examined the topoisomer distributions generated by topoisomerase I relaxation of paranemic RecA−DNA complexes formed by nontelomeric, telomeric G-rich, and telomeric C-rich single strands with

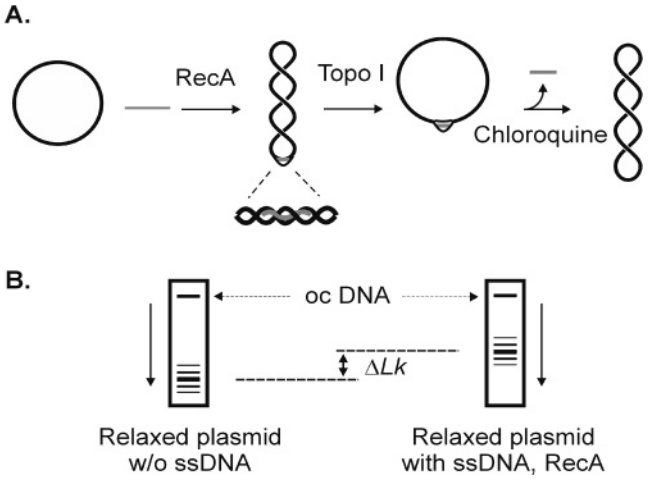

FIGURE 2: Schematic diagram of the RecA-mediated strand invasion assay. (A) Incubation of relaxed plasmid DNA with a ssDNA-containing RecA filament results in the formation of a paranemic ssDNA−dsDNA complex bound to RecA. Relaxation of this complex with topoisomerase I removes extraneous supercoils from the locally underwound paranemic complex. The change in DNA twist attributable to the paranemic complex is revealed by agarose gel electrophoresis in the presence of the intercalator chloroquine, which is present at sufficiently high concentrations in the gel to generate positive supercoiling and attendant loss of ssDNA. (B) Measurement of the linking difference (ΔLk) by agarose gel electrophoresis. The distribution of topoisomers is quantitated from digital images of lanes corresponding to samples relaxed in the presence and absence of ssDNA−RecA complexes. The values of Lk used in computing ΔLk are those corresponding to the most probable topoisomer in each distribution. The position of the open circular DNA band is indicated by oc.

homologous double-stranded sequences in plasmids containing telomeric repeat sequences (Figure 3). Control topoisomer distributions for the target plasmid were obtained from mock reactions that included all of the components of strand-exchange reactions except for ssDNA. Striking differences in the average values of ΔLk were observed between nontelomeric controls and RecA−DNA complexes containing either G-rich or C-rich single strands. Homologous pairing within the RecA strand-exchange complex results in strong duplex unwinding that is a linear function of the length of homologous DNA (*4*, *35*). A plot of ΔLk as a function of the size of the homologous region (Figure 4) gives a linear plot with a slope equal to the reciprocal of the helical repeat within the RecA−DNA complex and a *y*-intercept that gives the change in DNA twist due to helical distortion at the boundaries of the complex.

Our results with nontelomeric ssDNAs yielded an estimate for the helical repeat of the RecA−DNA complex that is close to the canonical value of 18.5 bp per turn and consistent with previously determined values (*4*, *36*). The residual homology length-independent value of ΔLk measured for the invasion of nontelomeric DNA was also nearly identical to the previously reported value, which corresponds to a reduction in DNA twist of nearly two helical turns (*4*).

Topoisomerase I relaxation of paranemic-joint complexes containing either G- or C-rich telomeric single strands gave values of $-\Delta Lk$ that were consistently and markedly lower than those measured for nontelomeric DNA strands similar in length. A plot of $-\Delta Lk$ versus the extent of homology for G- and C-rich single strands gave a value for the slope similar to that obtained for nontelomeric sequences. This indicates that the helical repeat of the RecA−DNA complex formed with telomeric single strands does not differ appreciably from that of nontelomeric sequences. However, the homology length-independent value of $-\Delta Lk$ found for both G- and C-rich telomeric repeats was 0.3 turn, approximately one-sixth of the nontelomeric value. Our interpretation of this result is that an essentially constant length of telomeric ssDNA amounting to 1.7 turns of B-form duplex DNA does not participate in strand invasion of the target molecule.

Stability and Polarity of Strand-Exchange Complexes. pRep90, target plasmid of the 100-nucleotide, G-rich telomeric ssDNA, has 16.5 tandem repeats of TTAGGG. Therefore, there are 16 possible invasion sites for the 100-nucleotide G-rich or C-rich ssDNAs, which would be expected to yield a heterogeneous population of strand-exchange intermediates. We examined whether the average values of ΔLk obtained in the topological assay were due to stochastic alignment of the invading strand, which could result from random invasion of the tandemly repeated ssDNA sequence in the various target sequence frames. The first approach that we used is a time-dependent assay. Previous studies reported that in the presence of either ATP or the nonhydrolyzable analogue ATPγS, RecA-mediated pairing of DNA repeats that results in suboptimal alignments is resolved in a time-dependent manner following an initial arbitrary mode of pairing (*37*, *38*). If the low values of ΔLk obtained for telomeric single strands relative to those measured for nontelomeric DNA strands similar in length were due to an initial arbitrary alignment of incoming single strands within the repeat sequence in the target plasmids, we expect that the topoisomer distribution of the target plasmid would change with time. We analyzed the topoisomer distribution of 100-nucleotide G-rich ssDNA pairing with pRep90 with the pairing step carried out for intervals between 1 and 5 h. Figure 5 shows that the plasmid topoisomer distribution was independent of time over this range, indicating that RecA-mediated alignment of the 100-nucleotide G-rich ssDNA reached a steady state within the first hour of the pairing reaction. Therefore, the ΔLk values obtained are likely to reflect an optimized alignment of telomeric single strands during pairing with target duplexes.

Second, we aimed to limit the initial mode of invasion of the repetitive sequences to a unique, single site on the plasmid. We used our asymmetric PCR procedure to make chimeric 158-nucleotide single-stranded DNAs consisting of 100 nucleotides of G-rich telomeric repeats fused to 58 nucleotides of flanking, nontelomeric DNA at the 5′- or 3′-end of the single strand (100G58N5′ or 100G58N3′, respectively; see Figure 1C). The nontelomeric extensions are homologous to sequences located at either the 5′- or 3′-boundaries of the telomeric repeat sequence in the target plasmid. The expected consequence of the nontelomeric flanking sequences was that alignment of the incoming single strand would be forced to occur in register with the first telomeric repeat next to the nontelomeric target sequence in the plasmid duplex. Previous reports indicate that the 58-nucleotide nontelomeric extension is above the size threshold for ssDNA molecules capable of forming stable strand invasion complexes in the presence of RecA and ATPγS (*39*).

Using the topological parameters deduced in Figure 4, the expected ΔLk shift for these 158-nucleotide constructs should

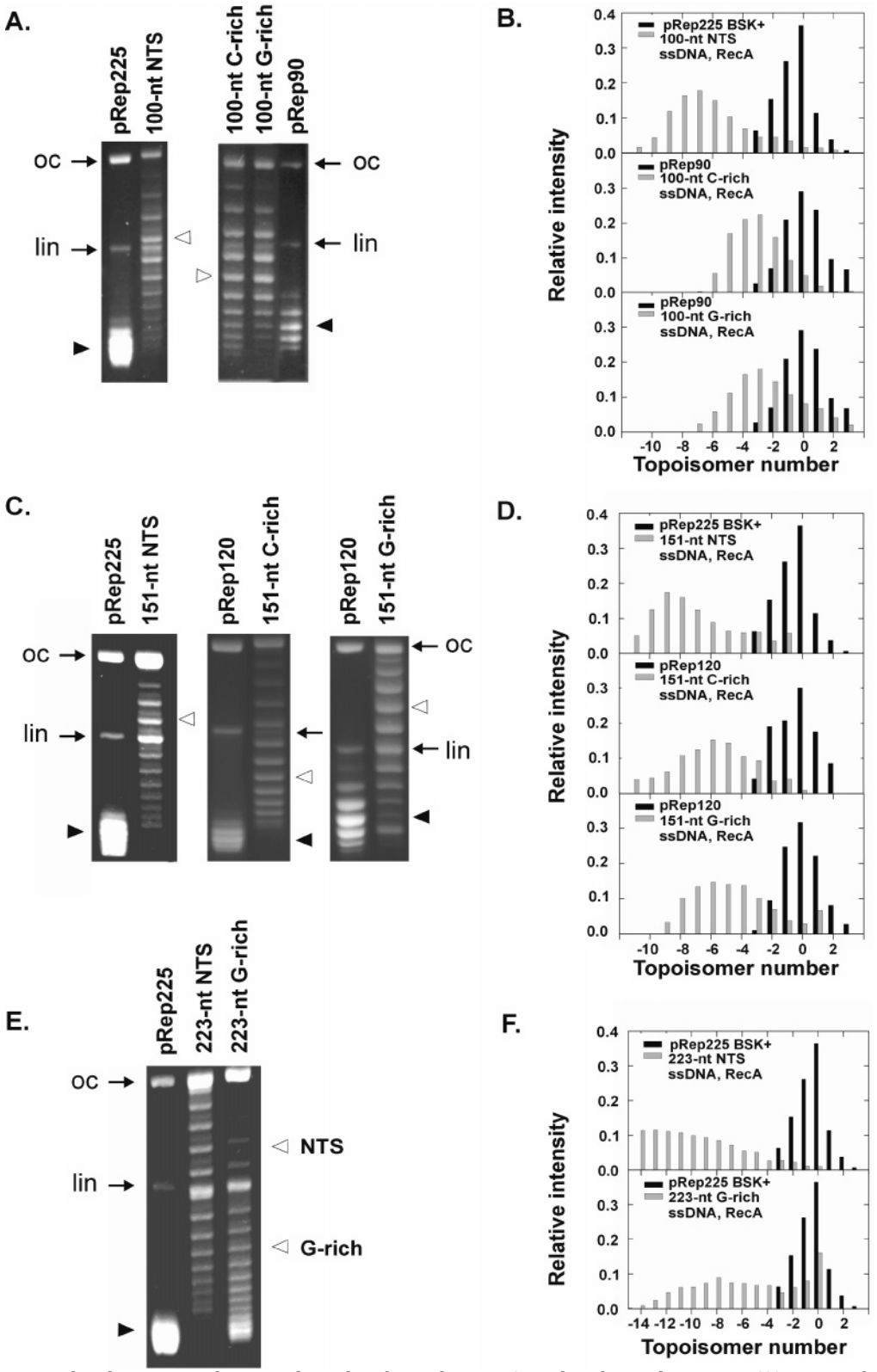

FIGURE 3: Topoisomer distributions in telomeric plasmids subjected to RecA-mediated strand invasion. (A) Digitized gel image of the topoisomer distributions of pRep225 BSK+ in the presence and absence of a homologously paired 100-nucleotide nontelomeric ssDNA−RecA complex (left) and of pRep90 in the presence and absence of a 100-nucleotide C-rich or G-rich telomeric ssDNA−RecA complex (right). The position of the most probable topoisomer in the free plasmid distribution is indicated by the black triangle; positions of the most probable topoisomer belonging to the strand invasion complexes are indicated by the white triangle. Note that the position of relative positions of the most probable topoisomer in each distribution may have been obtained from several gels that contained different concentrations of chloroquine (see Experimental Procedures). (B) Quantitated topoisomer distributions of the data shown in panel A. (C) Gel images of topoisomer distributions observed for plasmid pRep225 BSK+ in the presence and absence of a homologously paired 151-nucleotide nontelomeric ssDNA−RecA complex (left) and for plasmid pRep120 with RecA−ssDNA complexes containing either 151-nucleotide C-rich or G-rich ssDNA (right). (D) Quantitated topoisomer distributions of the data in panel C. (E and F) Gel images and topoisomer distribution data for plasmid pRep225 BSK+ with RecA−ssDNA complexes containing either 223-nucleotide nontelomeric or G-rich ssDNA. Positions of open circular and linear bands are indicated by oc and lin, respectively.

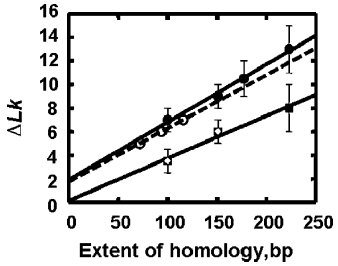

FIGURE 4: Dependence of Δ*Lk* induced by RecA-mediated strand invasion as a function of the length of ssDNA homologous to telomeric repeat-containing plasmids. The linking-number change (Δ*Lk*) was defined as the difference in *Lk* values corresponding to the most probable topoisomer in plasmid populations relaxed in the presence and absence of ssDNA−RecA filaments, respectively. The topoisomer distributions for all RecA complexes were centered at *Lk* values that were less than those of the native plasmid alone and thus gave uniformly negative values for Δ*Lk*: (●) nontelomeric DNA sequence data, (○) data of Kiianitsa and Stasiak (*4*), (■) G-rich telomeric repeat data, and (◇) C-rich telomeric repeat data. The best-fit length dependencies of Δ*Lk* for nontelomeric and telomeric sequences (both G-rich and C-rich) are given by the solid lines; the best fit to the data of Kiianitsa and Stasiak (*4*) is given by the dashed line.

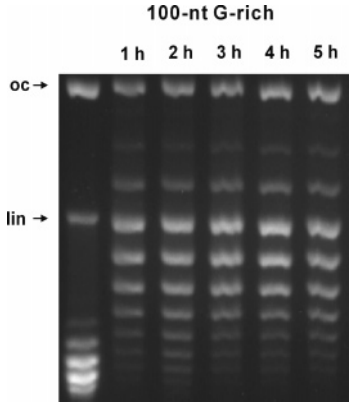

FIGURE 5: Time course of telomeric strand alignment by RecA. Topological unwinding assay of the pRep90 telomeric plasmid in the presence and absence of the homologously paired 100-nucleotide G-rich strand. RecA-coated single strands were incubated with the relaxed pRep90 at a ratio of 1:5 (plasmid:nucleoprotein filament). The pairing reaction was carried out for up to 5 h, after which complexes were treated with topoisomerase I at 37 °C for 1 h. Complexes were deproteinized with phenol, and topoisomers were analyzed by electrophoresis for 24 h in 1.3% agarose gels run in TBE buffer containing 0.5 μg/mL chloroquine phosphate.

correspond to unwinding by approximately 7 helical turns; this is simply the weighted average of contributions from 100 nucleotides of G-rich telomeric sequence and 58 nucleotides of nontelomeric DNA. In the absence of any asymmetry in the strand invasion complex, this shift should be the same independent of whether the nontelomeric extension is located at the 3′- or 5′-end of the telomeric single strand. Figure 6A shows the topoisomer distribution of strand-exchange complexes formed with 100G58N5′. The Δ*Lk* shift obtained for this construct agrees with the expected value of approximately −7. We obtained a similar effect on Δ*Lk* with a 209-nucleotide ssDNA composed of 151 nucleotides of G-rich telomeric repeats and 58 nucleotides of nontelomeric homologous DNA at the 5′-end (data not shown). The 209-nucleotide construct gave a Δ*Lk* shift equal to −9.5, again equal to the weighted Δ*Lk* value predicted from the properties of telomeric and nontelomeric ssDNA.

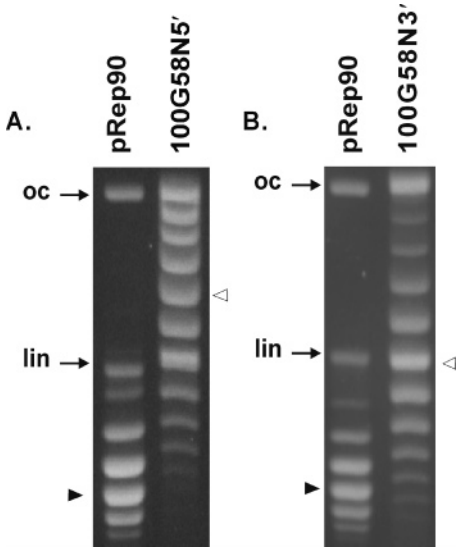

FIGURE 6: Unwinding induced by 158-nucleotide G-rich single strands with nontelomeric extensions. (A) Agarose gel analysis of pRep90 unwinding induced by pairing of a chimeric 158-nucleotide single strand, 100G58N3′, consisting of a 100-nucleotide segment of G-rich telomeric repeats and a 58-nucleotide nontelomeric 3′-extension (see Figure 1C). (B) Agarose gel analysis of the 158-nucleotide 5′-chimera, 100G58N5′. Both reactions were carried out under our standard strand-exchange assay conditions. Reaction products were run for 24 h in 1.3% agarose gels in TBE buffer containing 0.9 μg/mL chloroquine phosphate.

These results indicate that the differences in Δ*Lk* obtained for telomeric sequences were due to intrinsic properties of these sequences rather than random alignment between the incoming single strand and multiple repeats in the duplex−DNA target.

In contrast, when we repeated the same assay using the 158-nucleotide ssDNA consisting of 100 nucleotides of G-rich telomeric sequence and a 58-nucleotide, nontelomeric 3′-extension (100G58N3′), the observed Δ*Lk* shift was −4 turns, virtually identical to that of the 100-nucleotide G-rich single strand without the extension (Figure 6B). This can be explained if unwinding of the homologous sequence in the plasmid duplex was caused by pairing of either the telomeric or nontelomeric portions of the invading single strand, but the value is inconsistent with homologous pairing along the entire length of the single strand.

DMS Probing. Experiments designed to investigate the nuclease sensitivity of ssDNA−RecA and three-stranded RecA synaptic complexes were unsuccessful, probably due to protection of the DNA strands from enzymatic activity (data not shown). We therefore used chemical modification by dimethyl sulfate (DMS) to interrogate the structure of telomeric RecA-mediated paranemic-joint complexes. DMS predominantly methylates the N7 position of guanine, a position that is protected from methylation in some DNA triple helices and also in G-quartet (G4) structures (*40*−*42*). Methylation of the N3 positions of adenine and cytosine also occurs through DMS modification, although to a much lower extent. Previous studies with DMS have shown that the N7 position of G is susceptible to DMS attack in the ssDNA−RecA complex, the dsDNA−RecA complex, and all three strands involved in RecA-mediated D-loop structures (*6*, *8*, *43*). These data indicate that, relative to free DNA, G residues in ssDNA−RecA and dsDNA−RecA complexes show an

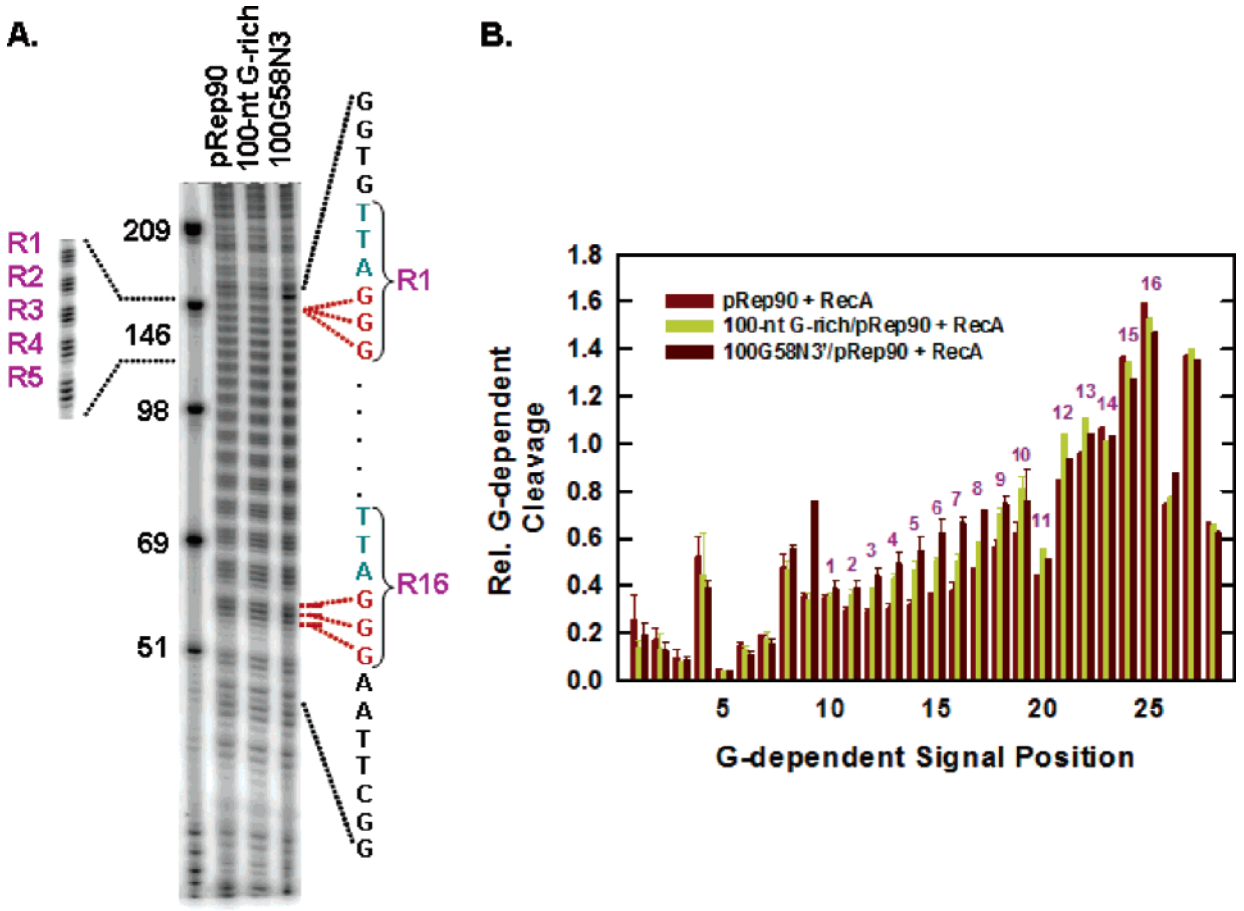

FIGURE 7: DMS sensitivity assays of RecA-mediated synaptic complexes. Autoradiogram of a 8% polyacrylamide sequencing gel showing the results of DMS sensitivity experiments carried out on the displaced G-rich strand of RecA synaptic complexes formed by telomeric single strands. (A) pRep90 was paired with 100-nucleotide G-rich telomeric or 158-nucleotide 3′-chimeric sequences (100G58N3′), treated with DMS, and cleaved with piperidine (see Experimental Procedures). Parallel application of samples to the gel took place after different detention times (the electrophoresis pattern shown in the inset corresponds to a lane that was run 120 min longer than those in the main figure). Bands resulting from G-specific cleavage are labeled according to the location of their respective telomeric repeat elements; the first repeat at the 5′-end of the G-rich duplex strand is designated R1. A reference ladder of telomeric single strands made by asymmetric PCR methods is shown in the far left lane with the sizes of the ssDNA (in nucleotides) as indicated. (B) Relative DMS accessibility of guanine residues spanning the repeat region plotted as a function of G residue location. The intensity of each G-specific band was determined relative to that of a reference G position located outside the region of homology (see Experimental Procedures). Cleavage signals arising from guanine tracts within individual telomeric repeats were summed for each repeat element and are plotted as a single data value located at the position of the central G residue. Representative error bars, indicating one standard deviation, are shown in cases for which three or more replicate values were available. Telomere repeat numbers shown in panel A are indicated above the corresponding peaks in the histogram.

up to 2-fold increase in reactivity to DMS. G residues in all three DNA strands present in RecA-mediated D-loop structures display a more modest 25−30% increase in DMS reactivity (*43*).

To test the accessibility of G residues in telomeric repeat-containing paranemic-joint complexes to methylation by DMS, synaptic complexes were made by incubating pRep90 with presynaptic complexes containing either the 100-nucleotide G-rich or 100G58N3′ strand (Figure 1C). Complexes were treated with DMS and deproteinized, and the DNA was cleaved with piperidine after labeling the displaced G-rich duplex strand with ^{32}P. To resolve the G-dependent cleavage pattern over the entire telomeric sequence tract, samples were subjected to electrophoresis for different periods of time from 50 to 170 min. As a control, a mock reaction mixture consisting of the target plasmid and all components except ssDNA was probed using the identical protocol. Figure 7A shows the resulting cleavage patterns of the G-rich strand in the target duplex. Bands were mapped to the corresponding region in the plasmid sequence and quantitated from the digital autoradiogram. The intensity of each band (normalized to the intensity of a G band located 25 bp outside the area of interest) revealed that a subset of G residues in the homologous region were up to 30% more susceptible to piperidine cleavage and hence more strongly modified by DMS (Figure 7B). Enhancement of methylation in both the 100-nucleotide G-rich and 100G58N3′ synaptic complexes was limited to the telomeric repeat region extending from the 5′-end of the displaced strand past the middle of the synaptic complex. None of the G residues located in the last three repeats at the 3′-end of the telomeric sequence exhibited enhancement in reactivity to DMS relative to those residues in the control plasmid. Moreover, homologous G residues located in the contiguous 3′-nontelomeric sequence of the 158 bp 3′-chimera showed no changes in reactivity relative to that in the plasmid alone, suggesting that those G residues in both cases participate in normal base pairing interactions. In contrast, quantitative

probing of G reactivity using the 100-nucleotide nontelomeric single strand, 100-nucleotide NTS, showed a similar 30% increase in reactivity to DMS across the entire homologous region in the plasmid duplex (see the Supporting Information). These results suggest that, on average, only 13 of the 16 complete telomeric repeats located in plasmid duplex participate in the paranemic-joint complex and that the three motifs located at the 3′-end or contiguous sequence elements that are located 3′ to this region are not involved in formation of a continuous synaptic filament.

Stimulation of Plasmid Dimerization by Telomeric Paranemic-Joint Complexes. Previous studies have reported that plasmids containing telomeric sequences show a tendency to aggregate under some solution conditions (*44*, *45*). Under our plasmid storage conditions, we find that such aggregation is a slow process that occurs on the time scale of weeks. In all of the experiments described here, we used the monomeric forms of these plasmids exclusively, which were separated from any residual higher-order forms by agarose gel electrophoresis (see Experimental Procedures). The purified plasmid DNA was used within 24 h; storage of plasmid DNAs in TE buffer during this brief period was accompanied by no detectable evidence of aggregation or formation of higher-order complexes. However, we observed the presence of DNA bands of reduced mobility in strand-exchange experiments that were carried out with G- and C-rich telomeric single strands. These low-mobility bands have the same mobility as noncovalent plasmid dimers and multimers generated by long-term storage of the telomeric repeat-bearing plasmids, and are consistent with the noncovalent association of single plasmid molecules in forming higher-order structures (Figure 8).

We investigated this phenomenon further by using ^{32}P-labeled ssDNA in strand-exchange assays under our standard reaction conditions. RecA protein was removed prior to electrophoresis, and in the presence of levels of chloroquine too low to destabilize the triple-helical complex ([chl] = 0−0.3 μg/mL), we observed monomeric, dimeric, and higher-order plasmid structures in the case of strand invasion by either G- or C-rich single strands (Figure 8). Higher chloroquine concentrations disrupt the strand invasion complex via high levels of positive supercoiling (through reductions in DNA twist), which drives dissociation of these multimeric structures (data not shown). Such higher-order structures were never observed with strand invasion complexes containing nontelomeric single strands, as shown in Figure 8.

Because telomeric sequences consist of tandemly repeated elements, there is an increased probability of multiple single strands invading the target duplex relative to nonrepetitive ssDNA. The relative probability of realizing multiple invasion events with repetitive ssDNA versus a unique strand-exchange intermediate is difficult to estimate, particularly since RecA-mediated strand invasion with circular single-stranded substrates has shown that strand invasion does not require a free single-strand end (*46*). Moreover, intermolecular strand invasion can occur in principle with both repetitive and nonrepetitive single strands whenever the target duplex is present in multiple copies (*47*−*54*). However, we took several steps to minimize the potential for multiple invasion events. First, we carried out titration experiments to determine the minimum molar ratio of presynaptic complex to target duplex that successfully depleted the free plasmid topoisomer population to negligible levels. The optimum ratio of presynaptic complex to target was found to be 5:1 for both telomeric and nontelomeric ssDNA (data not shown). Second, we reduced the likelihood of forming intermolecular strand-exchange complexes via plasmid−plasmid association by omitting K^+ and Na^+ ions in the strand-exchange buffer, which can promote the aggregation of plasmids through interactions involving polypurine/polypyrimidine sequences or G4 structures (*42*, *55*). Under these conditions, controls involving invasion of nontelomeric single-stranded DNA with plasmids bearing telomeric repeats showed no evidence of plasmid dimers or higher-order structures (Figure 8). This suggests that G- and C-rich paranemic-joint complexes exert specific effects on the formation of higher-order plasmid structures under solution conditions that do not favor the formation of higher-molecular weight species.

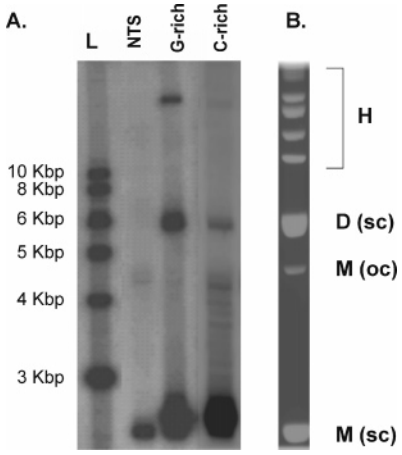

FIGURE 8: Noncovalent association of plasmids promoted by formation of telomeric strand invasion complexes. Telomeric and nontelomeric paranemic-joint complexes containing ^{32}P-labeled single-stranded DNA were prepared in the presence of RecA protein. After deproteinization, the multistranded complexes were analyzed by electrophoresis in 1.3% agarose gels in the absence of chloroquine. (A) Phosphorimager scan of ^{32}P-labeled paranemic-joint molecules formed by 151-nucleotide single strands with plasmid pRep120: L, 1 kb ladder standards; NTS, 151-nucleotide nontelomeric control; and G-rich, 151-nucleotide, G-rich telomeric single strand. Lane-to-lane variations in product intensities are likely due to sequence-dependent differences in the stability of strand-exchange intermediates in the absence of RecA (*10*, *11*, *39*). (B) Agarose gel (1.3%) separation of higher-order forms of pRep120 obtained by prolonged storage and visualized by staining with ethidium bromide. Association states of different species are as indicated: M(sc), supercoiled monomer; M(oc), nicked monomer; and D(sc), supercoiled dimer. Bands collectively labeled H consist of nicked dimer and other higher-order forms.

DISCUSSION

Little is known about the behavior of repeated sequence DNA in RecA-mediated strand exchange. To better understand general mechanistic aspects of homologous pairing involving repetitive DNA sequences, we have examined aspects of DNA structure in RecA-mediated strand exchange involving defined single-stranded human telomeric sequences. We have used *E. coli* RecA protein in our studies, as opposed to its human homologue, hRad51, for several reasons. First, these strand-exchange systems are essentially identical with respect to the structure of the intermediate

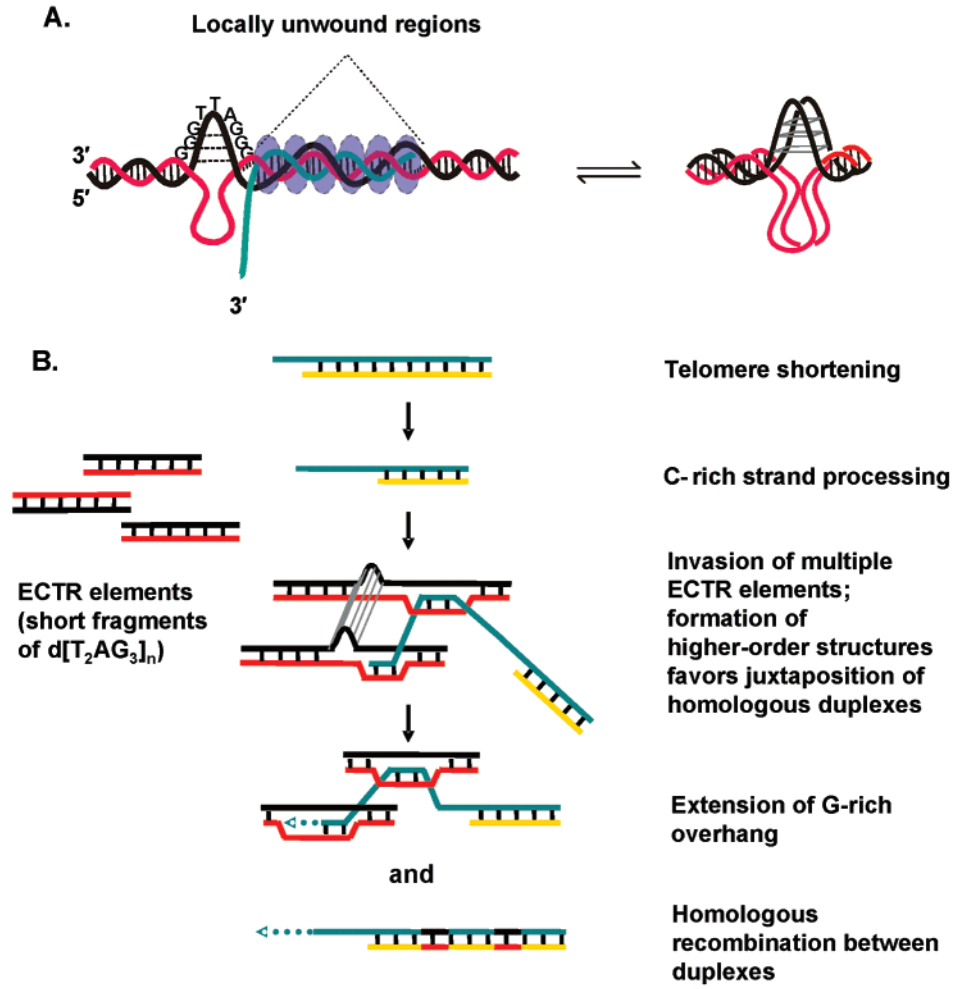

FIGURE 9: (A) Proposed secondary and higher-order structures induced by telomeric single-strand invasion. The G-rich telomeric duplex strand is colored black, the C-rich repeat strand red, and the invading telomeric repeat strand (G-rich in this case) green. The RecA filament is shown as an array of dashed ellipses. Formation of G·G base pairs along the G-rich strand takes place (indicated by horizontal dashed lines connecting G residues), accompanied by unwinding of the complementary sequence in the C-rich strand, depicted as an unpaired loop or as an extrahelical duplex structure. Local duplex unwinding may occur in addition to the formation of the G·G paired loop, and this is indicated by broken base pairs in the figure. Formation of multimers, demonstrated in Figure 8, could be mediated by interactions between G·G loops, but might also involve G·C base pairing interactions involving unpaired residues in the C-rich strand. The invading single strand has been omitted in the right-hand figure for clarity. (B) A model for telomere maintenance in ALT Cells. Diagrammatic representation of proposed steps involved in telomere maintenance via homologous recombination. Telomere G-rich and C-rich strands are shown in green and yellow, respectively; the color coding of other strands follows that in panel A. Processing of the C-rich strand may lengthen the G-rich overhang to promote subsequent strand-exchange steps (*64*). Rad51 and associated factors facilitate invasion of the G-rich overhang into multiple telomeric duplexes, such as those present on extrachromosomal telomeric repeats (ECTRs). Lengthening of the telomeric duplex region can then occur through multiple homologous recombination events with extension of the 3′-overhang occurring via an independent leading strand synthesis pathway.

nucleoprotein filament and employ closely similar mechanisms of strand exchange. Second, the biological context of hRad51 and the role of accessory factors in strand exchange remain highly controversial (*56*). Indeed, the kinetics of strand exchange observed with purified Rad51 from either yeast or human sources are significantly slower than that of RecA in vitro; this may be due to the absence of accessory factors that are present in the in vivo strand-exchange complex (*57*). Our choice of RecA is therefore motivated by the need for a well-defined system, which is essential to uncovering the molecular mechanisms of sequence-dependent strand exchange. Finally, in vivo studies of recombination in or near repeated sequence elements in *E. coli* cells have provided insight into the biological basis of instability in repeat-containing loci present in the human genome (*14*). By examining RecA−DNA structural intermediates in a well-characterized, model in vitro system, we may uncover universal aspects of homologous strand exchange that are relevant for telomere maintenance.

Using a topological method, we examined the shift in the topoisomer distribution (ΔLk) of paranemic complexes formed by single-stranded telomeric DNAs with homologous duplex DNA. The topological results indicate that the helical repeat of the RecA−DNA ternary complexes containing telomeric single-stranded DNA does not differ significantly from that of nontelomeric sequences. We therefore conclude that the local helicity of telomeric strand-exchange complexes is similar to that postulated for nontelomeric DNA, namely, a triple-helical structure in which all strands have a helical repeat of approximately 18−20 residues per turn. However, relative to nontelomeric DNA, telomeric sequences show a constant and reproducible offset in the dependence of ΔLk on the length of the homologous region. This offset is equal to 1.7 turns of B-form DNA or, all other factors being equal,

~3 of the hexamer repeats that comprise the human telomeric sequence. The simplest interpretation of our results is therefore that on the order of three duplex telomeric repeats, on average, do not participate in formation of the RecA paranemic-joint complex. These repeat elements may be driven into an alternative DNA conformation, perhaps involving G·G base pairing, by the strong unwinding activity of the RecA presynaptic filament. Similar shifts in ΔLk values were obtained using both C-rich and G-rich telomeric single strands (Figures 3 and 4), suggesting that the sequence-dependent effects are not specifically due to sequence-dependent differences in DNA structure within the RecA−DNA filament.

Additional topological experiments with chimeric single strands composed of a fixed length of telomeric sequence and a 58-nucleotide segment of homologous nontelomeric DNA located at either the 5′- or 3′-end suggest that there is a stability bias inherent in the binding of the 5′- and 3′-ends of the single-stranded telomeric sequence. The 5′-region of the invading chimeric sequence is evidently more tightly associated with the RecA synaptic complex than is the 3′-end of the single strand. The fact that there is a stability bias that favors association of the 5′-region of the repeat sequence relative to the 3′-end suggests that the 3′-end of the telomeric synaptic complex (relative to the invading ssDNA) is more dynamic and may be available for targeting additional duplex sequence elements. These conclusions are further supported by methylation protection data that are consistent with unperturbed levels of DMS modification in the region that is apparently excluded from invasion.

Remarkably, our experiments indicate a propensity for target plasmids to form multimers in strand-exchange reactions that involve telomeric single strands. This effect was specific to strand invasion complexes formed using telomeric ssDNA and was never observed with nontelomeric ssDNA. A previous report that RecA presynaptic filaments are capable of forming higher-order complexes with duplex DNA (*58*) also suggested a connection between levels of homologous pairing and plasmid−plasmid association. However, results from electron microscopy suggested that those RecA-mediated aggregates were essentially nonspecific and, unlike the higher-order complexes reported here, do not require telomeric repeat sequences (*59*).

A recent study by Duquette et al. (*60*) showed that the strong unwinding activity accompanying in vitro and in vivo transcription can drive G- and C-rich tracts, including human telomeric DNA sequences, into loops that contain G4 structures. This finding is notably consistent with our proposal that RecA-dependent unwinding leads to alternative helical structures in telomeric duplexes. However, the fact that *both* G-rich and C-rich RecA complexes exhibit behavior different from that of nontelomeric strand invasion complexes strongly suggests that this putative alternative structure is formed outside the paranemic complex. We considered scenarios in which unwinding generates an altered helical structure at a boundary of the paranemic complex and displaces a corresponding length of invading ssDNA. Assuming identical values for the helical repeat of telomeric and nontelomeric paranemic complexes, the observed residual twist difference of +1.7 turns between these complexes is probably too small to be consistent with formation of an intramolecular G4 structure. However, our measured twist difference can easily be accommodated by alternative structures containing intramolecular G·G base pairs belonging to two successive repeats. The unusual propensity for plasmid molecules containing strand invasion complexes to form dimeric plasmid structures could be consistent with an equilibrium involving intermolecular association of G·G pairs to form G4 structures (Figure 9A). Similar intermolecular interactions involving association of G·G base pairs (*61*) and other repeated sequence motifs (*62*) have been reported.

Bechter et al. (*63*) have shown that the increased levels of recombination observed in human ALT cells are a telomere-specific phenomenon as distinguished from a nonspecific increase in homologous recombination level that affects all chromosomal loci. Our finding that RecA-mediated invasion of telomeric single strands does not result in a fully paired synaptic complex along with the observation that telomeric synaptic complexes favor plasmid−plasmid association suggests a model for ALT-dependent telomere maintenance via homologous recombination (Figure 9B). Pairing of telomeric duplexes may be favored by the association of G·G pairs in forming G4 structures. If the 3′-end of the presynaptic complex is free, this end could invade a second duplex, facilitating homology searches during homologous recombination. Such structures may be themselves quite dynamic and may provide additional mechanisms for extending the 3′-telomeric overhang by DNA replication. Alternatively, homologous recombination between extrachromosomal telomeric sequences (ECTRs) and the chromosomal telomeric duplex may account for the increased variation in telomere length observed in ALT-dependent cells.

ACKNOWLEDGMENT

We thank Drs. Woodring Wright and Jerry Shay for their generous gifts of telomeric sequence-containing plasmids and in particular for helpful discussions. We are grateful to Dr. Wright and also to Drs. Jonathan Chaires, Richard Sinden, Dipankar Sen, and Jungwei Chen for their respective comments on an earlier version of the manuscript. Also, we thank Dr. Alexandre Vetcher for help and guidance with DMS probing experiments.

SUPPORTING INFORMATION AVAILABLE

Data concerning the DMS reactivity of RecA-mediated synaptic complexes formed on nontelomeric sequences (Figure S1). This material is available free of charge via the Internet at http://pubs.acs.org.

REFERENCES

1. Howard-Flanders, P., West, S. C., and Stasiak, A. (1984) Role of RecA protein spiral filaments in genetic recombination, *Nature 309*, 215−220.
2. Flory, J., Tsang, S. S., and Muniyappa, K. (1984) Isolation and visualization of active presynaptic filaments of recA protein and single-stranded DNA, *Proc. Natl. Acad. Sci. U.S.A. 81*, 7026−7030.
3. Rosselli, W., and Stasiak, A. (1990) Energetics of RecA-mediated recombination reactions. Without ATP hydrolysis RecA can mediate polar strand exchange but is unable to recycle, *J. Mol. Biol. 216*, 335−352.
4. Kiianitsa, K., and Stasiak, A. (1997) Helical repeat of DNA in the region of homologous pairing, *Proc. Natl. Acad. Sci. U.S.A. 94*, 7873−7840.

5. Wong, B. C., Chiu, S.-K., and Chow, S. A. (1998) The role of negative superhelicity and length of homology in the formation of paranemic joint promoted by RecA protein, *J. Biol. Chem. 273*, 12120−12127.
6. Di Capua, E., and Müller, B. (1987) The accessibility of DNA to dimethylsulfate in complexes with recA protein, *EMBO J. 6*, 2493−2498.
7. Dombroski, D. F., Scraba, D. G., Bradley, R. D., and Morgan, A. R. (1983) Studies of the interaction of RecA protein with DNA, *Nucleic Acids Res. 11*, 7487−7504.
8. Leahy, M. C., and Radding, C. M. (1986) Topography of the interaction of recA protein with single-stranded deoxyoligonucleotides, *J. Biol. Chem. 261*, 6954−6960.
9. Kowalczykowski, S. C., and Eggleston, A. K. (1994) Homologous pairing and DNA strand-exchange proteins, *Annu. Rev. Biochem. 63*, 991−1043.
10. Tracy, R. B., and Kowalczykowski, S. C. (1996) *In vitro* selection of preferred DNA pairing sequences by the *Escherichia coli* RecA protein, *Genes Dev. 10*, 1890−1903.
11. Tracy, R. B., Baumohl, J. K., and Kowalczykowski, S. C. (1997) The preference for GT-rich DNA by the yeast Rad51 protein defines a set of universal pairing sequences, *Genes Dev. 11*, 3423−2431.
12. Dixon, D. A., and Kowalczykowski, S. C. (1991) Homologous pairing *in vitro* stimulated by the recombination hotspot, Chi, *Cell 66*, 361−371.
13. Jeffreys, A. J., Wilson, V., and Thein, S. L. (1985) Hypervariable "minisatellite" regions in human DNA, *Nature 314*, 67−73.
14. Napierala, M., Dere, R., Vetcher, A., and Wells R. D. (2004) Structure-dependent recombination hot spot activity of GAA·TTC sequences from intron 1 of the Friedriech's ataxia gene, *J. Biol. Chem. 279*, 6444−6454
15. Baird, D. M., Colman, J., Rosser, Z. H., and Royle, N. J. (2000) High levels of sequence polymorphism and linkage disequilibrium at the telomere of 12q: Implications for telomere biology and human evolution, *Am. J. Hum. Genet. 66*, 235−250.
16. Wilkie, A. O., Higgs, D. R., Rack, K. A., Buckle, V. J., Spurr, N. K., Fischel-Ghosdian, N., Ceccherini, I., Brown, W. R., and Harris, P. C. (1991) Stable length polymorphism of up to 260 kb at the tip of the short arm of human chromosome 16, *Cell 64*, 595−606.
17. Shay, J. W., and Wright, W. E. (1996) Telomerase activity in human cancer, *Curr. Opin. Oncol. 8*, 66−71.
18. Saretzki, G. (2003) Telomerase inhibition as cancer therapy, *Cancer Lett. 194*, 209−219.
19. Cerone, M. A., Londono-Vallejo, J. A., and Bacchetti, S. (2001) Telomere maintenance by telomerase and by ALT can coexist in human cells, *Hum. Mol. Genet. 10*, 1945−1952.
20. Yeager, T. R., Neumann, A. A., Englezou, A., Huschtscha, L. I., Noble, J. R., and Reddel, R. R. (1999) Telomerase-negative immortalized cells contain a novel type of promyelocytic (PML) body, *Cancer Res. 59*, 4175−4179.
21. Wu, G., Lee, W. H., and Chen, P. L. (2000) NBSI and TRF1 colocalize at promyelocytic leukemia bodies during late S/G2 phases in immortalized telomerase-negative cells, *J. Biol. Chem. 275*, 30618−30622.
22. Grobelny, J. V., Godwin, A. K., and Broccoli, D. (2000) ALT-associated PML bodies are present in viable cells and are enriched in cells in G2/M phase of the cell cycle, *J. Cell Sci. 113*, 4577−4585.
23. Benson, F. E., Stasiak, A., and West, S. C. (1994) Purification and characterization of the human Rad51 protein, an analogue of *E. coli* RecA, *EMBO J. 13*, 5764−5771.
24. Yu, X. S., Jacobs, A., West, S. C., Ogawa, T., and Egelman, E. H. (2001) Domain structure and dynamics in the helical protein filaments formed by RecA and Rad51 on DNA, *Proc. Natl. Acad. Sci. U.S.A. 98*, 8419−8424.
25. Baumann, P., and West, S. C. (1997) The human Rad51 protein: Polarity of strand transfer and stimulation by hRP-A, *EMBO J. 16*, 5198−5206.
26. Sherman, F., and Roman, H. (1963) Evidence for two types of allelic recombination in yeast, *Genetics 48*, 253−271.
27. Konforti, B. B., and Davis, R. W. (1987) 3′ homologous free ends are required for stable joint molecule formation by the RecA and single-stranded binding proteins of *Escherichia coli*, *Proc. Natl. Acad. Sci. U.S.A. 84*, 690−694.
28. Konforti, B. B., and Davis, R. W. (1990) The preference for a 3′ homologous end is intrinsic to RecA-promoted strand exchange, *J. Biol. Chem. 265*, 6916−6920.
29. Moyzis, R. K., Buckingham, J. M., Cram, L. S., Dani, M., Deaven, L. L., Jones, M. D., Meyne, J., Ratliff, R. L., and Wu, J.-R. (1988) A highly conserved repetitive DNA sequences, $(TTAGGG)_n$, present at the telomeres of human chromosomes, *Proc. Natl. Acad. Sci. U.S.A. 85*, 6622−6626.
30. Sambrook, J., Fritsch, E. F., and Maniatis, T. (1989) *Molecular cloning: A laboratory manual*, Cold Spring Harbor Laboratory Press, Plainview, NY.
31. Worcel, A., Strogatz, S., and Riley, D. (1981) Structure of chromatin and the linking number of DNA, *Proc. Natl. Acad. Sci. U.S.A. 78*, 1461−1465.
32. Prunell, A. (1998) A topological approach to nucleosome structure and dynamics: The linking number paradox and other issues, *Biophys. J. 74*, 2531−2544.
33. Schutte, B. C., and Cox, M. M. (1988) Homology-dependent underwinding of duplex DNA in recA protein generated paranemic complexes, *Biochemistry 27*, 7886−7894.
34. Julin, D. A., Riddles, P. W., and Lehman, I. R. (1986) On the mechanism of pairing of single- and double-stranded DNA molecules by the recA and single-stranded DNA-binding proteins of *Escherichia coli*, *J. Biol. Chem. 261*, 1025−1030.
35. Cai, L., Marquardt, U., Zhang, Z., Taisey, M. J., and Chen, J. (2001) Topological testing of the mechanism of homology search promoted by RecA protein, *Nucleic Acids Res. 29*, 1389−1398.
36. Stasiak, A., and Di Capua, E. (1982) The helicity of DNA in complexes with recA protein, *Nature 299*, 185−186.
37. Sen, S., Karthikeyan, G., and Rao, B. J. (2000) RecA realigns suboptimally paired frames of DNA repeats through a process that requires ATP hydrolysis, *Biochemistry 39*, 10196−10206.
38. Navadgi, V. M., Sen, S., and Rao, B. J. (2002) RecA-promoted sliding of base pairs within DNA repeats: Quantitative analysis by a slippage assay, *Biochem. Biophys. Res. Commun. 296*, 983−987.
39. Hsieh, P., Camerini-Otero, C. S., and Camerini-Otero, R. D. (1992) The synapsis event in the homologous pairing of DNAs: RecA recognizes and pairs less than one helical repeat of DNA, *Proc. Natl. Acad. Sci. U.S.A. 89*, 6492−6496.
40. Hanvey, J. C., Shimizu, M., and Wells, R. D. (1990) Site-specific inhibition of *Eco*RI restriction/modification enzymes by a DNA triple helix, *Nucleic Acids Res. 18*, 157−161.
41. Collier, D. A., Mergny, J.-L., Thoung, N. T., and Helene C. (1991) Site-specific intercalation at the triplex−duplex junction induces a conformational change which is detectable by hypersensitivity to diethylpyrocarbonate, *Nucleic Acids Res. 19*, 4219−4224.
42. Balagurumoorthy, P., and Brahmachari, S. K. (1994) Structure and stability of human telomeric sequence, *J. Biol. Chem. 269*, 21858−21869.
43. Adzuma, K. (1992) Stable synapsis of homologous DNA molecules mediated by the *Escherichia coli* RecA protein involves local exchange of DNA strands, *Genes Dev. 6*, 1679−1694.
44. Voloshin, O. N., Veselkov, A. G., Belotserkovskii, B. P., Danilevskaya, O. N., Pavlova, M. N., Dobrynin, V. N., and Frank-Kamenetskii, M. D. (1992) An eclectic DNA structure adopted by human telomeric sequence under superhelical stress and low pH, *J. Biomol. Struct. Dyn. 9*, 643−652.
45. Huertas, D., Lipps, H., and Azorin, F. (1994) Characterization of the structural conformation adopted by $(TTAGGG)_n$ telomeric DNA repeats of different length in closed circular DNA, *J. Biomol. Struct. Dyn. 12*, 79−90.
46. Cox, M. M. (1999) Recombinational DNA repair in bacteria and the RecA protein, *Prog. Nucleic Acid Res. Mol. Biol. 63*, 311−366.
47. Holmes, V. F., Scandellari, F., Benjamin, K. R., and Cozzarelli, N. R. (2002) Structure of reaction intermediates formed during *Saccharomyces cerevisiae* Rad51-catalyzed strand transfer, *J. Biol. Chem. 277*, 38945−38953.
48. Mcllwraith, M. J., Van Dyke, E., Masson, J. Y., Stasiak, A. Z., Stasiak, A., and West, S. C. (2000) Reconstitution of the strand invasion step of double-strand break repair using human Rad51 Rad52 and RPA proteins, *J. Mol. Biol. 304*, 151−164.
49. Menetski, J. P., Bear, D. G., and Kowalczykowski, S. C. (1990) Stable DNA heteroduplex formation catalyzed by the *Escherichia coli* RecA protein in the absence of ATP hydrolysis, *Proc. Natl. Acad. Sci. U.S.A. 87*, 21−25.
50. Shibata, T., DasGupta, C., Cuningham, R. P., Williams, J. G., Osber, L., and Radding, C. M. (1981) Homologous pairing in genetic recombination, *J. Biol. Chem. 256*, 7565−7572.
51. West, S. C., Cassuto, E., and Howard-Flanders, P. (1981) recA protein promote homologous-pairing and strand-exchange reac-

tions between duplex DNA molecules, *Proc. Natl. Acad. Sci. U.S.A. 78*, 2100−2104.
52. Cox, M. M., and Lehman, I. R. (1981) Directionality and polarity in recA protein-promoted branch migration, *Proc. Natl. Acad. Sci. U.S.A. 78*, 6018−6022.
53. DasGupta, C., and Radding, C. M. (1982) Polar branch migration promoted by recA protein: Effect of mismatched base pairs, *Proc. Natl. Acad. Sci. U.S.A. 79*, 762−766.
54. Holmes, V. F., Benjamin, K. R., Crisona, N. J., and Cozzarelli, N. R. (2001) Bypass of heterology during strand transfer by *Saccharomyces cerevisiae* Rad51 protein, *Nucleic Acids Res. 29*, 5052−5057.
55. Goobes, R., Cohen, O., and Minskey, A. (2002) Unique condensation patterns of triplex DNA: Physical and physiological implications, *Nucleic Acids Res. 30*, 2154−2161.
56. Sung, P., Krejci, L., Van Komen, S., and Sehorn, M. G. (2003) Rad51 recombinase and recombination mediators, *J. Biol. Chem. 278*, 42729−42732.
57. Baumann, P., Benson, F. E., and West, S. C. (1996) Human Rad51 protein promotes ATP-homologous pairing and strand transfer reactions *in vitro*, *Cell 87*, 757−766.
58. Tsang, S. S., Muniyappa, K., Azhderian, E., Gonda, D. K., Radding, C. M., Flory, J., and Chase, J. W. (1985) Intermediates in homologous pairing promoted by recA protein: Isolation and characterization of active presynaptic complexes, *J. Mol. Biol. 185*, 295−309.
59. Biet, E., Sun, J. S., and Dutreix, M. (2003) Stimulation of D-loop formation by polypurine/polypyrimidine sequences, *Nucleic Acids Res. 31*, 1006−1012.
60. Duquette, M. L., Handa, P., Vincent, J. A., Taylor, A. F., and Maizels, N. (2004) Intracellular transcription of G-rich DNAs induces formation of G-loops, novel structures containing G4 DNA, *Genes Dev. 18*, 1618−1629.
61. Venczel, E. A., and Sen, D. (1996) Synapsable DNA, *J. Mol. Biol. 257*, 219−224.
62. Sinden, R. R., Potaman, V. N., Oussatcheva, E. A., Pearson, C. E., Lyubchenko, Y. L., and Shlyakhtenko, L. S. (2002) Triplet repeat DNA structures and human genetic disease: Dynamic mutations from dynamic DNA, *J. Biosci. 27*, 53−65.
63. Bechter, O., Zou, Y., Shay, J. W., and Wright, W. E. (2003) Homologous recombination in human telomerase-positive and ALT cells occurs with the same frequency, *EMBO Rep. 4*, 1138−1143.
64. Huffman, K. E., Levene, S. D., Tesmer, V. M., Shay, J. W., and Wright (2000) Telomere shortening is proportional to the size of the G-rich telomeric 3′-overhang, *J. Biol. Chem. 275*, 19719−19722.

BI047735R